Highly Efficient Conformer-Specific Adiabatic Cis → Trans Photoisomerization of *cis*-1-(2-Anthryl)-2-phenylethene in S_1

Jack Saltiel,* Yuxin Zhang, and Donald F. Sears, Jr.

Contribution from the Department of Chemistry, The Florida State University, Tallahassee, Florida 32306-3006

Received May 19, 1995[⊗]

Abstract: Emission from *cis*-1-(2-anthryl)-2-phenylethene, *c*-APE, in toluene consists primarily (up to 76%) of fluorescence from adiabatically formed ^{1} *t*-APE_B*. In this respect, the behavior of *c*-APE is analogous to that of the naphthyl analogue, *c*-NPE. However, the conformer specific adiabatic photoisomerization, ^{1}*c*-APE_B* → ^{1}*t*-APE_B*, is much more efficient in *c*-APE than in *c*-NPE (≥44% vs ≥2%) although the lifetime of ^{1}*c*-APE_B* is 1000-fold longer than the lifetime of ^{1}*c*-NPE_B* (4.5 ± 0.5 ns vs 4 ± 1 ps). Resolution of the spectra of ^{1}*c*-APE* and ^{1}*t*-APE_B* was achieved by application of principal component analysis on a matrix of sets of fluorescence spectra measured in the presence of Ar, air, and O_2. The known fluorescence spectrum of *t*-APE_B and the known Stern−Volmer constant for O_2 quenching of the fluorescence of *t*-APE_B serve as the constraints for this resolution. Sequential quenching by O_2 of ^{1}*c*-APE_B* and ^{1}*t*-APE_B* is reflected in a quadratic Stern−Volmer plot for the latter.

Introduction

cis-1-(2-Anthryl)-2-phenylethene, *c*-APE, has attracted a great deal of attention because it belongs to a family of 1,2-diarylethenes that exhibits one way cis → trans adiabatic photoisomerization on the lowest triplet energy surface.[1] In contrast to the triplet state where the transoid geometry represents a readily accessible global energy minimum, the energy surface of the lowest excited singlet state has been postulated to have deep minima at transoid and cisoid geometries and to undergo no photoisomerization in either direction.[1−3] This was presumably consistent with different fluorescence spectra[2,4] and large fluorescence quantum yields from solutions of the two isomers.[2,3] Following direct excitation, photoisomerization in the cis → trans direction was assumed to involve ^{1}*c*-APE* → ^{3}*c*-APE* intersystem crossing as the initial key step.[2,3] This assumption was based in part on transient triplet−triplet absorption measurements that have led to $\phi_{is} = 0.17$ as the estimated intersystem crossing yield of ^{1}*c*-APE*.[3] Semiempirical quantum mechanical calculations suggest that the perpendicular geometry, ^{1}p*, in the APE_A conformer is a transition state along the ^{1}c* → ^{1}t* reaction coordinate that lies 16 and 23 kcal/mol higher than ^{1}c* and ^{1}t*, respectively.[5] Relatively large energy barriers for ^{1}c* → ^{1}p* and ^{1}t* → ^{1}p* torsional motion were attributed to confinement of the electronic excitation largely in the anthracenyl moiety of the two isomers.[1,5]

This study was prompted by recent reports showing that adiabatic ^{1}c* → ^{1}t* isomerization of aryl substituted olefins is much more common than previously imagined.[6−10] Observations showing that the inefficient (∼0.2%) adiabatic photoisomerization of *cis*-stilbene[8] is enhanced at least 10-fold (∼2%) when a 2-naphthyl group is substituted for one of the phenyl groups[10] and is rendered highly efficient (∼61%) when an even larger aryl group, the 1-pyrenyl, is used instead[9] raise doubts concerning the validity of the conclusion that the ^{1}c* → ^{1}t* pathway does not contribute to the photoisomerization of *c*-APE.[1−3] Following the submission of this work we became aware of a brief report of observations on *c*-APE in methylcyclohexane/3-methylpentane (MCH-3MP) solutions by Mazzucato and co-workers that led to the proposal that the singlet adiabatic photoisomerization pathway is dominant at least for temperatures higher than room temperature.[11,12]

Experimental Section

Materials. Toluene (Fisher, HPLC grade) was washed with several portions of concentrated sulfuric acid, several portions of water, and aqueous sodium bicarbonate. It was then dried over sodium sulfate and distilled. Quinine sulfate (Matheson, Coleman and Bell, reagent) was recrystallized three times from water. A mixture of *c*- and *t*-APE was synthesized by a Wittig reaction as previously described.[13] Separation of the two isomers was achieved by column and rotary chromatography and the structure of *c*-APE was confirmed by ^{1}H NMR (300 MHz, $DCCl_3$) δ 6.70−6.83 (dd, 2 H, J = 12.5 Hz, vinyl), 7.22−7.25 (m, 3 H), 7.31−7.34 (m, 3 H), 7.44−7.46 (m, 2 H), 7.78−7.81 (d, 1 H, J = 9 Hz), 7.90 (s, 1 H), 7.96−7.98 (m, 2 H), 8.30 (s, 1 H), 8.34 (s, 1 H).

Spectroscopic Measurements. Absorption spectra were measured using a Perkin-Elmer Lambda-5 spectrophotometer and fluorescence

[⊗] Abstract published in *Advance ACS Abstracts,* March 1, 1996.

(1) For a review see Arai, T.; Tokumaru, K. *Chem. Rev.* **1993**, *93*, 23−39.

(2) Karatsu, T.; Arai, T.; Sakuragi, H.; Tokumaru, K. *Chem. Phys. Lett.* **1985**, *115*, 9−15.

(3) Arai, T.; Karatsu, T.; Tsuchiya, M.; Sakuragi, H.; Tokumaru, K. *Chem. Phys. Lett.* **1988**, *149*, 161−166.

(4) Castel, N.; Fischer, E. *J. Photochem. Photobiol. A* **1989**, *48*, 109−114.

(5) Bartocci, G.; Masetti, F.; Mazzucato, U.; Spalletti, A.; Orlandi, G.; Poggi, G. *J. Chem. Soc., Faraday Trans. 2* **1988**, *84*, 385−399.

(6) (a) Sandros, K.; Becker, H.-D. *J. Photochem.* **1987**, *39*, 301−315. (b) Görner, H. *J. Photochem. Photobiol. A* **1988**, *43*, 263−288. (c) Sandros, K.; Becker. H.-D. *J. Photochem. Photobiol. A* **1988**, *43*, 291−292.

(7) (a) Sandros, K.; Sundahl, M.; Wennerström, O.; Norinder, U. *J. Am. Chem. Soc.* **1990**, *112*, 3082−3086. (b) Sandros, K.; Sundahl, M.; Wennerström, O. *J. Phys. Chem.* **1993**, *97*, 5291−5294. (c) Sandros, K.; Sundahl, M. *J. Phys. Chem.* **1994**, *98*, 5705−5708.

(8) (a) Saltiel, J.; Waller, A.; Sun, Y.-P; Sears, D. F., Jr. *J. Am. Chem. Soc.* **1990**, *112*, 4580−4581. (b) Saltiel, J.; Waller, A. S.; Sears, D. F., Jr. *J. Photochem. Photobiol. A: Chem.* **1992**, *65*, 29−40. (c) Saltiel, J.; Waller, A. S.; Sears, D. F., Jr. *J. Am. Chem. Soc.* **1993**, *115*, 2453−2465.

(9) Spalletti, A.; Bartocci, G.; Mazzucato, U.; Galiazzo, G. *Chem. Phys. Lett.* **1991**, *186*, 297−302.

(10) Saltiel, J.; Tarkalanov, N.; Sears, D. F., Jr. *J. Am Chem. Soc.* **1995**, *117*, 5586−5587.

(11) Mazzucato, U.; Spalletti, A.; Bartocci, G. *Coord. Chem. Rev.* **1993**, *125*, 251−260.

(12) We thank Professor U. Mazzucato for bringing ref 11 to our attention.

(13) Maercker, A. *Org. React.* **1965**, *14*, 270−490

0002-7863/96/1518-2811$12.00/0 © 1996 American Chemical Society

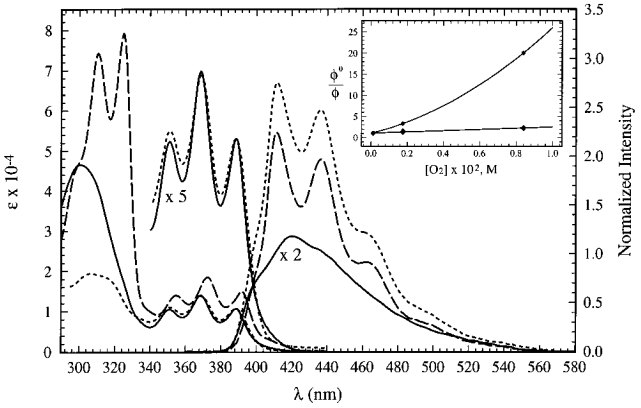

Figure 1. Absorption spectra of *c*-APE (—) and *t*-APE (— —) and fluorescence excitation spectrum (λ_{em} = 415 nm) of *c*-APE (- - -) and contributions of ^{1}*t*-APE$_B$* (— —) and ^{1}*c*-APE* (×2) (—) emissions in *c*-APE fluorescence (λ_{exc} = 366 nm) (- - -) in toluene at 20 °C. All fluorescence spectra are corrected for nonlinearity in instrumental response. Inset: Global Stern−Volmer plots for the O_2 effect on resolved fluorescence areas of *c*-APE and *t*-APE$_B$.

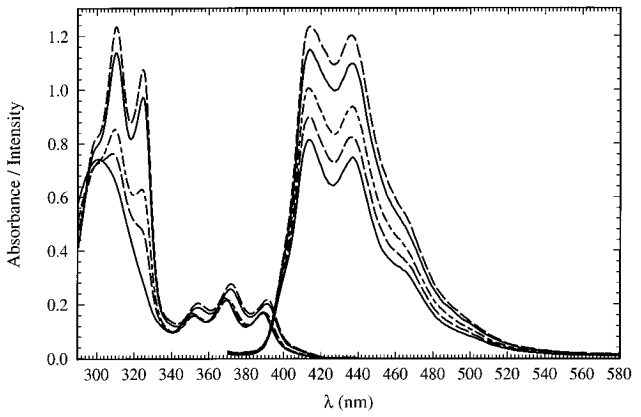

Figure 2. Absorption and fluorescence spectra of a solution of *c*-APE in toluene after irradiation at 20 °C in a static cell at 366 nm for 0, 5, 10, 30, and 40 min, bottom to top.

spectra were measured using an extensively modified Hitachi/Perkin-Elmer MPF-2A spectrophotometer as previously described.[14] ^{1}H NMR spectra were obtained on a Gemini 300 MHz instrument.

Fluorescence Lifetimes. Fluorescence lifetimes were measured using a SPEX Fluorolog fluorimeter.[15]

Data Analysis. Principal component analyses with self-modeling (PCA-SM) calculations were performed on a PC's limited Dell 80486/87 (25 MHz) microcomputer as previously described.[14]

Results

Static Cell Experiments. The UV spectra of *c*- and *t*-APE in toluene are compared in Figure 1. Figure 2 shows absorption and fluorescence spectra of a solution of *c*-APE in Ar-saturated toluene irradiated at 20.0 °C with 366-nm (nearly an isosbestic point of the APE isomers) light in a 1-cm static cell in our fluorimeter for different time intervals. While the buildup of *t*-APE is obvious in the absorption spectra, the corresponding change in the fluorescence spectra is an increase in intensity with no readily discernible difference in spectral shape. Quantitative treatment of the changes in absorption in Figure 2 was achieved using PCA. No self-modeling is involved as both pure APE isomer spectra are known, Figure 1. Irradiation for 40 min in the fluorimeter resulted in 69% conversion of *c*-APE to

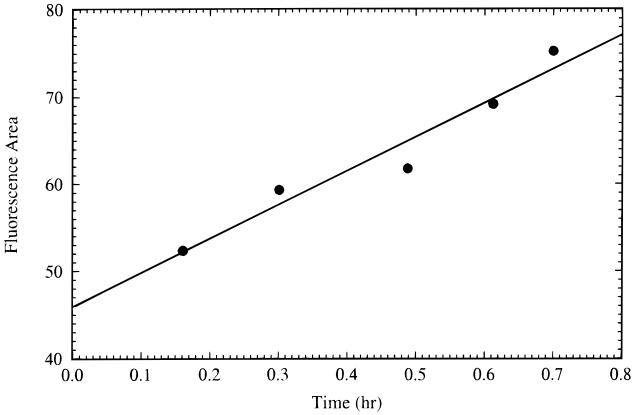

Figure 3. Adherence of the time evolution of fluorescence areas in Figure 2 to eq 1.

t-APE with a corresponding 50% increase in fluorescence spectrum intensity. The time dependence of the mixture fluorescence quantum yield, $\bar{\phi}_f$, is given by

$$\bar{\phi}_f(t) = \bar{f}_c(t)\bar{\phi}_{f_c} + \bar{f}_t(t)\bar{\phi}_{f_t} = \bar{\phi}_{f_c} + (\bar{\phi}_{f_t} - \bar{\phi}_{f_c})\bar{f}_t(t) \qquad (1)$$

where $\bar{\phi}_{f_t}$ and $\bar{\phi}_{f_c}$ are the effective fluorescence quantum yields of *t*- and *c*-APE at the λ_{exc} employed and

$$\bar{f}_t(t) = \frac{\bar{\epsilon}_t(\lambda_{exc})\bar{c}_t}{\bar{\epsilon}(\lambda_{exc})\bar{c}} = 1 - \bar{f}_c(t) \qquad (2)$$

represents the fraction of *t*-APE molecules excited at time *t*. Following correction for the very small increases in absorbance at 366 nm with time, the plot of fluorescence area vs $\bar{f}_t(t)$ obeys eq 1, Figure 3. Fluorescence area extrapolation to $\bar{f}_t$ values of 0 and 1 gives $\bar{\phi}_{f_t}/\bar{\phi}_{f_c}$ = 1.80. Bars over the symbols indicate that the quantities reflect the behavior of mixtures of conformers for each isomer.

Flow Cell Experiments. To minimize interference by *t*-APE photoproduct formed in the course of the measurements, fluorescence spectra were also recorded at 20.0 °C in toluene using a flow cell system as described for *cis*-stilbene.[8] Under these conditions, it was shown with the aid of neutral density filters (up to a factor of 5 attenuation) that the dependence of fluorescence intensity from a *c*-APE solution on incident excitation intensity is strictly linear. Ar-, air- and O_2-saturated solutions ([*c*-APE] = 3.4 × 10^{-5} M, 150 mL) were employed and a minimum number of fluorescence spectra recorded at λ_{exc} = 374, 384, 395, 399, 403, 405, 407, and 409 nm. The small *c*-APE absorbances at $\lambda_{exc} \geq$ 399 nm gave rise to relatively weak and noisy fluorescence spectra that contain large scattered light contributions. These spectra were not of sufficiently good quality to be employed in the analysis. A second experiment was therefore carried out employing a higher *c*-APE concentration, 1.4 × 10^{-4} M. Approximately 200 mL of this solution, saturated successively with Ar, O_2, and air, was circulated through the flow cell system and spectra were recorded for 370 $\leq \lambda_{exc} \leq$ 410 nm. Better quality fluorescence spectra were obtained at the expense of onset distortion due to self-absorption. In a similar experiment an APE solution composed of 5% *t*-APE and 95% *c*-APE was employed, [APE] = 1.1 × 10^{-4} M, in order to evaluate the effect of *t*-APE contamination on the fluorescence spectra. Pure solvent background spectra were employed for baseline correction. Negligible buildup of *t*-APE was established by comparing absorption and fluorescence-excitation spectra of working solutions before and after measurement of fluorescence spectra. The fluorescence spectra of Ar-saturated *c*-APE solutions bear a strong similarity to the

(14) Saltiel, J.; Sears, D. F., Jr.; Choi, J.-O.; Sun, Y.-P.; Eaker, D. W. *J. Phys. Chem.* **1994**, *98*, 35−46.

(15) We thank Professor M. Kasha for the use of this instrument and Dr. Juan-Carlos Del Valle for assistance in carrying out the measurements.

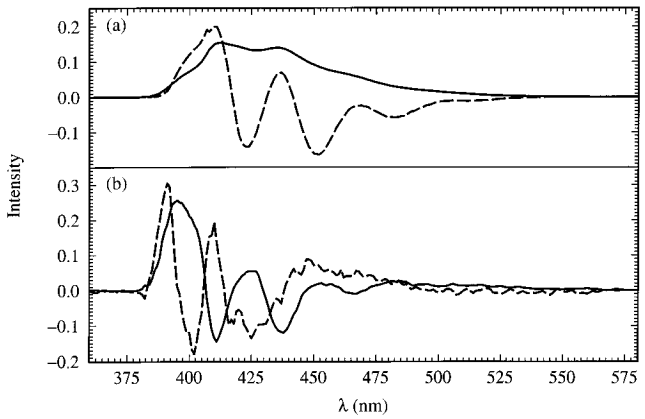

Figure 4. Eigenvectors of the global matrix consisting of fluorescence spectra from all three flow cell experiments and the resolved *t*-APE$_A$ and *t*-APE$_B$ spectra from ref 18: (a) V_α (—), V_β (− −); (b) V_γ (—), V_δ (− −). The six largest eigenvalues were 5.407×10^{-1}, 4.632×10^{-3}, 6.442×10^{-4}, 8.507×10^{-5}, 7.617×10^{-6}, and 5.310×10^{-6}, respectively.

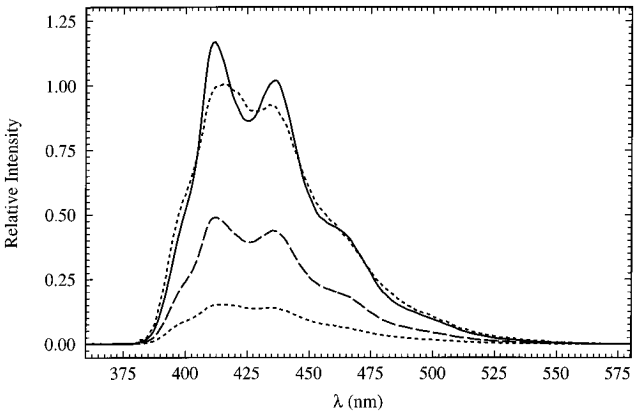

Figure 5. A typical set of fluorescence spectra of *c*-APE (1.4×10^{-4} M) in Ar- (—), air- (− −) and O_2-saturated (- - -) toluene solution obtained for $\lambda_{exc} = 390$ nm. The spectrum for the O_2-saturated solution is also shown multiplied by a factor of 6.64 (the area ratio). The spectra are corrected for background and self-absorption, but not for nonlinearity of instrumental response.

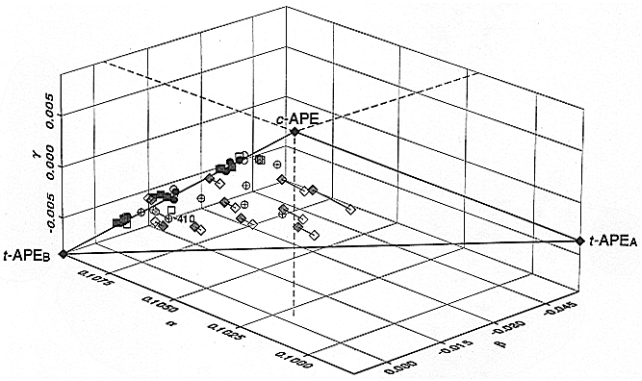

Figure 6. Combination coefficients for the global matrix corresponding to the eigenvectors in Figure 4 in α, *β*, *γ* space. Experimental spectra for [*c*-APE] = 3.4×10^{-5} and 1.4×10^{-4} M solutions are designated by squares and circles, respectively; spectra for the *c*-APE solution contaminated by 5% *t*-APE are designated by open diamonds, and their projection on the three-component plane by shaded diamonds. Projections are on the normals to the plane; the apparent angle of the lines to the plane is an optical illusion due to coordinate scale selection. The cross within the symbol designates spectra for $\lambda_{exc} \geq 400$ nm and closed circles and squares correspond to the 18 spectra employed in the two-component treatment.

resolved fluorescence spectrum of *t*-APE$_B$,[5,16−18] whereas fluorescence-excitation spectra roughly track the absorption spectrum of *c*-APE, Figure 1. The fluorescence spectrum broadens with increasing [O_2].

Spectral Resolution. Fluorescence spectra were corrected for self-absorption based on the effective transmittance of each APE solution. Satisfactory background corrections were achieved by subtraction of the corresponding solvent background spectrum, provided that the Rayleigh scattered-light peak from the solvent did not overlap the region of the fluorescence spectrum, $\lambda_{exc} \leq 375$ nm. Spectra for longer λ_{exc} were corrected by least-squares fitting of eigenvectors obtained from a matrix of spectra for $\lambda_{exc} \leq 375$ nm to the regions of each spectrum free of scattered-light peaks. This procedure allows reconstruction of the spectrum over the entire wavelength range. The spectral region requiring correction was then substituted into the experimental spectrum and the corrected spectrum was added to the matrix.[18a] Since each spectrum potentially consists of at least four components (*c*- and *t*-APE$_A$ and *c*- and *t*-APE$_B$), the final least-squares fit correction employed the four significant eigenvectors, Figure 4, from a matrix consisting of the flow cell spectra described above and the previously resolved pure component *t*-APE$_A$ and *t*-APE$_B$ fluorescence spectra.[18a] A set of typical spectra from this matrix (corrected for self-absorption and background emission, but not for nonlinearity of instrumental response) clearly shows the pronounced effect of oxygen on the fluorescence profile, Figure 5. Examination of a plot of the combination coefficients from this global matrix in α, *β*, *γ* space, Figure 6, shows that most spectra from the two pure *c*-APE solutions fall along a line that includes the combination coefficients of the spectrum of *t*-APE$_B$ at one end. Spectra corresponding to the solution containing 5% t-APE show strong systematic deviations from this line with points for spectra at the longest λ_{exc} and the largest [O_2] falling closest to the point defined by the combination coefficients of *t*-APE$_A$. Based on this behavior the PCA treatment was confined to the subset of 18 spectra from the pure *c*-APE solutions obtained with $\lambda_{exc} \leq$ 398 nm. The matrix spanned the 360−580-nm range in 1-nm increments. Eigenvalues and eigenvectors from this matrix are, to a very good approximation, consistent with a two component system, Figure 7. Using target analysis to define the combination coefficients of the known *t*-APE$_B$ spectrum as dot products of the spectrum with the eigenvectors in Figure 7 defines a point that falls on the normalization line, Figure 8, and corresponds to $K_{SV}^c = 175 \pm 7$ M^{-1} (see eq 4 below). It is in reasonable agreement with $K_{SV}^c = 145 \pm 16$ M^{-1} based on our fluorescence lifetime of ^{1}*c*-APE* and the assumption of identical O_2-quenching rate constants, $3.2_2 \times 10^{10}$ M^{-1} s^{-1},[18] for ^{1}*c*-APE* and ^{1}*t*-APE$_B$*.

Two extreme possibilities can be envisioned that would lead to strictly two-component fluorescence spectra from *c*-APE solutions. In both, ^{1}*t*-APE$_B$* fluorescence arises through its adiabatic formation from ^{1}*c*-APE$_B$*, Scheme 1; however, in the first possibility (case **a**) the second component is due entirely

(16) (a) Spalletti, A.; Bartocci, G.; Masetti, F.; Mazzucato, U.; Cruciani, G. *Chem. Phys.* **1992**, *160*, 131−144. (b) Bartocci, G.; Mazzucato, U.; Spalletti, A.; Elisei, F. *Spectrochim. Acta, A* **1990**, *46*, 413−418. (c) Bartocci, G.; Masetti, F.; Mazzucato, U.; Baraldi, I.; Fischer, E. *J. Mol. Struct.* **1989**, *193*, 173−183.

(17) (a) Ghiggino, K. P.; Skilton, P. F.; Fischer, E. *J. Am. Chem. Soc.* **1986**, *108*, 1146−1149. (b) Wismontski-Knittel, T.; Das, P. K.; Fischer, E. *J. Phys. Chem.* **1984**, *88*, 1163−1168. (c) Fischer, G.; Fischer, E. *J. Phys. Chem.* **1981**, *85*, 2611−2613.

(18) (a) Saltiel, J.; Zhang, Y.; Sears, D. F., Jr.; Choi, J.-O. *Res. Chem. Intermed.* **1995**, *21*, 899−921. (b) Adjustments for deviations from unity of the intercepts of Stern−Volmer plots have led to small increases in the Stern−Volmer constants reported in ref 18a.

Scheme 1

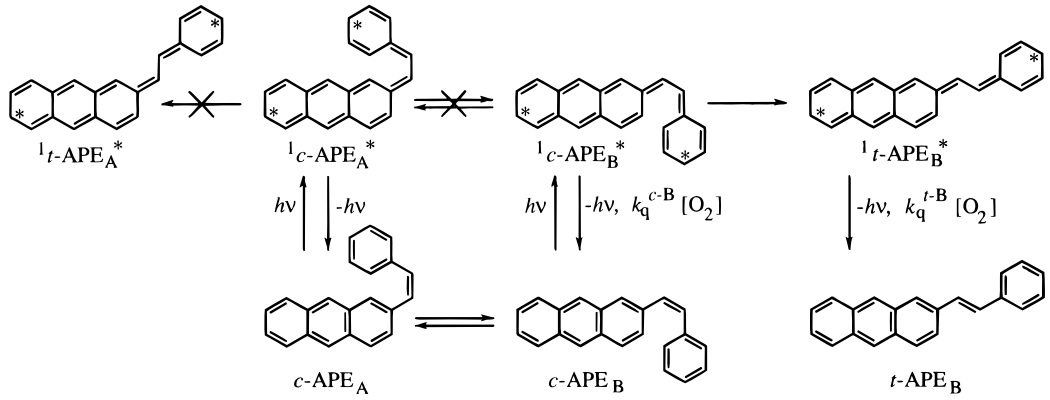

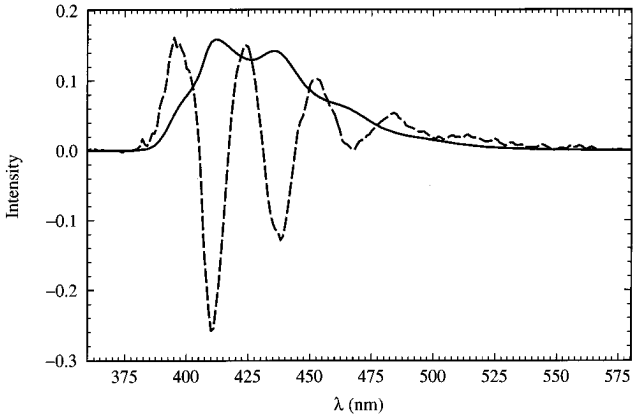

Figure 7. Eigenvectors of the matrix consisting of 18 fluorescence spectra of *c*-APE in toluene (3.4×10^{-5} and 1.4×10^{-4} M) obtained in the flow cell as a function of [O_2] for $\lambda_{exc} \leq 398$ nm. The four largest eigenvalues were 0.1366, 0.1964×10^{-3}, 0.2330×10^{-4}, and 0.9124×10^{-5}.

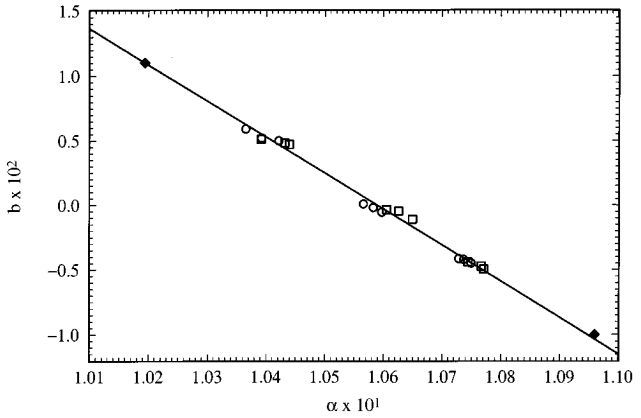

Figure 8. Normalization line based on the eigenvectors in Figure 7. Experimental combination coefficients and pure component combination coefficients are also shown (see Figure 6 for symbols).

to ^1c-APE$_A$* fluorescence, whereas in the second possibility (case **b**) it is due entirely to ^1c-APE$_B$* fluorescence. Based on case **a**, an attempt to find the combination coefficients for the fluorescence spectrum of *c*-APE by applying the Stern−Volmer constant criterion[14] on *t*-APE$_B$ fluorescence yielded an anomalously large apparent $K_{SV}^{t\text{-B}} = 1191 \pm 20$ M^{-1} value and a highly structured spectrum. The larger than expected O_2 effect on ^1t-APE$_B$* fluorescence intensity suggests prior quenching of the precursor ^1c-APE$_B$* excited state as shown in Scheme 1. Based on Scheme 1 the dependence of the fluorescence intensity of ^1t-APE$_B$* on [O_2] should follow the quadratic relationship

$$\left(\frac{\phi_{fo}}{\phi_f}\right)_{t\text{-B}} = (1 + K_{SV}^{c\text{-B}}[O_2])(1 + K_{SV}^{t\text{-B}}[O_2]) \qquad (3)$$

where $K_{SV}^{c\text{-B}}$ and $K_{SV}^{t\text{-B}}$ are the Stern−Volmer constants of ^1c- and ^1t-APE$_B$*, respectively. The value $K_{SV}^{t\text{-B}} = 900 \pm 25$ M^{-1} was determined previously.[18] However, the value obtained above for K_{SV}^{c} could, in principle, correspond to either ^1c-APE$_A$* or ^1c-APE$_B$*, or to both. The search for the combination coefficients of ^1c-APE* fluorescence was based on reproducing the oxygen effect defined by eq 3 (see inset, Figure 1), assuming, tentatively, that $K_{SV}^{c\text{-B}} = 160$ M^{-1}. The resulting resolved fluorescence spectrum is shown in Figure 1. If the two-component case **b** applied exclusively this spectrum could be assigned to ^1c-APE$_B$*. That this is not strictly correct is revealed by the λ_{exc} dependence of the combination coefficients on the normalization line in Figure 8. This topic is addressed in detail in the Discussion section.

Fluorescence Quantum Yields. Fluorescence quantum yields were determined for *c*-APE under flow cell conditions and for *t*-APE under static cell conditions using quinine bisulfate in 0.1 N H_2SO_4 as the fluorescence standard, $\phi_f = 0.546$.[19] Ar-saturated toluene solutions of the APE's at 20.0 °C were employed and absorbances of standard and unknown were matched at λ_{exc}. Slits were set at 3.0 nm for both excitation and emission monochromators. Fluorescence quantum yields, corrected for differences in index of refraction, are 0.52, 0.53, 0.49, 0.46, and 0.12 for *c*-APE excited at $\lambda_{exc} = 340$, 350, 360, 390, and 410 nm, respectively, and 0.89 for *t*-APE excited at either 340 or 344 nm. Estimated uncertainties in the quantum yields are ±3%.

Fluorescence Lifetimes. Fluorescence lifetimes of an Ar-outgassed toluene solution of *c*-APE, ~2.5×10^{-5} M, were measured at ambient temperature, ~27 °C, using the phase modulation method. Duplicate determination using short and long exposure times yielded clean biexponential decays corresponding to lifetimes of 27.9 ± 0.2 (95.0%) and 4.5 ± 0.5 ns (5.0%), for the major and minor components, respectively, $\chi^2 = 1.5$. These measurements were made with excitation and emission monochromators set at 325 and 420 nm, respectively.

Discussion

The UV absorption spectrum of *c*-APE in Figure 1 is in good agreement with an approximate spectrum of its methyl derivative, *cis*-1-(2-anthryl)-2-*p*-toluylethene (*c*-ATE), in MCH that was estimated by Castel and Fischer by subtracting the spectrum of *t*-ATE from the spectrum of a nearly equimolar mixture of

(19) Meech, S. R.; Phillips, D. *J. Photochem.* **1983** *23*, 193−217.

c- and *t*-ATE.[20] It is in excellent agreement with the spectrum of *c*-APE measured by Mazzucato, Spalletti, and Bartocci in methylcyclohexane/3-methylpentane (MCH-3MP) 9/1 (v/v).[11] Examination of Figures 1 and 2 shows that in toluene at 20.0 °C the fluorescence spectra of *c*- and *t*-APE are nearly identical, exhibiting only subtle differences. Since, provided $\lambda_{exc} \leq 395$ nm, the fluorescence of *t*-APE is due primarily to the *t*-APE_B conformer, this preliminary examination suggests *t*-APE_B as the major source of fluorescence following *c*-APE excitation. Support for this conclusion is provided by the observation that the lifetime, 27.9 ± 0.2 ns, of the major decay component of *c*-APE fluorescence in toluene corresponds exactly to the lifetime of the fluorescence of *t*-APE_B.[5,16a] The lifetime of the minor fluorescence component, 4.5 ± 0.5 ns, is nearly a factor of 2 smaller than the fluorescence lifetime of *t*-APE_A, 8.7 ± 0.5 ns.[5,16a] Thus, adiabatic ^{1}*c*-APE_A* → ^{1}*t*-APE_A* isomerization can be discounted as a significant process. Analogous observations led Mazzucato et al. to postulate adiabatic ^{1}*c*-APE_B* → ^{1}*t*-APE_B* isomerization in MCH-3MP.[11] However, in MCH-3MP the fluorescence spectrum of *c*-APE at 25 °C differs sharply from that of *t*-APE, whereas the spectra of the two isomers are very similar at 81 °C.[11]

PCA Resolution of *c*-APE Fluorescence. As described in the Results section, our resolution of *c*-APE fluorescence spectra in toluene into pure component spectra rests, in no small measure, on prior knowledge of an accurate *t*-APE_B fluorescence spectrum and of the corresponding Stern−Volmer quenching constant, $K_{SV}{}^{t\text{-B}}$. Two *t*-APE_B fluorescence spectra have been reported, both based on PCA-SM resolutions of matrices of *t*-APE fluorescence spectra in toluene at 20 °C.[16a,18a] They appear to differ mainly in the degree of definition of vibrational structure. We have traced the reason for the discrepancy to the difference in SM criteria employed in the two studies.[18a] Bartocci et al. relied on the Lawton and Sylvestre nonnegativity constraint[21] that gives a broad range of acceptable spectra for solutions,[16a] whereas our resolution was based on the Stern−Volmer constant[14] that gives a nearly unique solution, well within the range of acceptable spectra from the Lawton and Sylvestre approach.[18a] Since the outer limit Lawton and Sylvestre combination coefficients that were assigned by Bartocci et al. to *t*-APE_B are further out on the normalization line than the actual coefficients, their spectrum includes a substantial negative contribution of *t*-APE_A fluorescence leading to the impression of better-resolved vibronic structure. The consequence of using such a difference spectrum in the quantitative analysis of *c*-APE fluorescence spectra would be the erroneous conclusion that *t*-APE_A is present as a third component in the fluorescence of *c*-APE solutions. This conclusion is inconsistent with the PCA results and with the biexponential fluorescence decays observed here in toluene and in the Mazzucato et al. work in MCH-3MP.[11]

For a two-component system, the location of the combination coefficients ($\alpha_{t\text{-B}}$,$\beta_{t\text{-B}}$) of the fluorescence spectrum of *t*-APE_B on the normalization line in Figure 8 defines the Stern−Volmer constant of the cis component according to

$$\frac{F^o(\beta^o - \beta_{t\text{-B}})}{F(\beta - \beta_{t\text{-B}})} = 1 + K_{SV}{}^c[O_2] \qquad (4)$$

where F^o and F are areas of the fluorescence spectra (prior to normalization) and β^o and β are the corresponding coefficients of the normalized spectra in the absence and in the presence of O_2, respectively.[14] However, as pointed out in the Results section, if the spectra consisted only of ^{1}*c*-APE_B* and ^{1}*t*-APE_B* fluorescence, their combination coefficients would define only one point for each [O_2] on the normalization line, i.e., their position would be independent of λ_{exc}. This is based on the reasonable assumption that the efficiency of the adiabatic ^{1}*c*-APE_B* → ^{1}*t*-APE_B* process is λ_{exc} independent. It follows that the λ_{exc}-induced dispersion of the points on the normalization line in Figure 8 into well-defined regions for each [O_2] can be accounted for only if ^{1}*c*-APE_A* fluorescence is present as a component whose contribution varies with λ_{exc}. We conclude that despite the apparent behavior of the spectral matrix as a two-component system, each experimental spectrum contains fluorescence contributions from three excited species (^{1}*c*-APE_A*, ^{1}*c*-APE_B*, and ^{1}*t*-APE_B*), but that *c*-APE_A and *c*-APE_B have closely related fluorescence spectra and similar fluorescence lifetimes. The contribution of ^{1}c-APE_A* fluorescence is especially enhanced in spectra for $\lambda_{exc} \geq 400$ nm. Combination coefficients for these spectra fall closest to the *c*-APE corner (located by target analysis using the vectors in Figure 4 and the *c*-APE spectrum in Figure 1) of the *c*-APE/*t*-APE_B side of the triangle in Figure 6. Inclusion of these spectra into the spectral matrix does lead to eigenvectors and eigenvalues indicating the presence of a minor third component. When spectra from the solution contaminated with *t*-APE, $\lambda_{exc} \geq 400$ nm, are included, the spectral matrix becomes a four-component system. This is evident in Figure 6 where most relevant points lie in front of the three-component plane (triangle) and are shown together with their projections on that plane. Deviations from the plane increase with increasing [O_2]. They are a measure of the contribution of *c*-APE_A* fluorescence in the spectra.

To test the conclusion that the fluorescence spectra and lifetimes of the cis rotamers are nearly identical the PCA treatment was applied separately to each set of three fluorescence spectra obtained for each λ_{exc}. The results for $\lambda_{exc} = 374$ nm (low [c-APE]) and $\lambda_{exc} = 402$ nm (high [*c*-APE]) are typical. They are described here because based on the location of the combination coefficients of the two sets of spectra in the global plot in Figure 6 they represent nearly the widest variation in *c*-APE_A/*c*-APE_B fluorescence ratio that was achieved in the experimental spectra. Defining the location of ($\alpha_{t\text{-B}}$,$\beta_{t\text{-B}}$) on the normalization line of each matrix by target analysis resulted in $K_{SV}{}^c$ = 152 and 158 M^{-1} for λ_{exc} = 374 and 402 nm, respectively. Applying the quadratic relationship, eq 3, for the quenching of ^{1}*t*-APE_B* fluorescence gave the *c*-APE spectra shown in Figure 9. Clearly, increasing the contribution of ^{1}*c*-

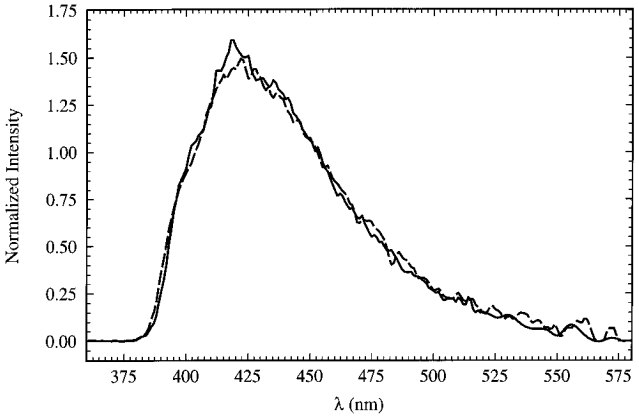

Figure 9. *c*-APE fluorescence spectra based on three-spectra sets for $\lambda_{exc} = 374$ nm (—, [*c*-APE] = 3.4 × 10^{-5} M) and $\lambda_{exc} = 402$ nm (− −, [*c*-APE] = 1.4 × 10^{-4} M).

(20) Castel, N.; Fischer, E. *J. Photochem. Photobiol. A* **1989**, *48*, 109−114.

(21) Lawton, W. H.; Sylvestre, E. A. *Technometrics* **1971**, *13*, 617−633.

(22) This conclusion is independent of the value of $\phi_{t\text{-B}}$ employed. Use of the earlier lower value[16a,18a] for $\phi_{t\text{-B}}$ in the above analysis would lead to a corresponding decrease in $\phi_{t\text{-B}}{}^c$.

APE_A* fluorescence in the spectra has little effect on K_{SV}^{c} and on the appearance of the *c*-APE fluorescence spectrum. Though subtle differences are discernible, the spectra in Figure 9 are nearly identical to the ^1c-APE* spectrum in Figure 1.

We are justified therefore in using eq 3 with $K_{SV}^{c\text{-}B} = 160$ M^{-1} and $K_{SV}^{t\text{-}B} = 900$ M^{-1}, based on the sequential excited state quenching shown in Scheme 1, to guide the search for the coefficients of the ^1c-APE* fluorescence spectrum. The fit to the expected quadratic Stern−Volmer plot (inset) and the corresponding resolved ^1c-APE* fluorescence spectrum are shown in Figure 1. The broad appearance of the spectrum is consistent with room temperature fluorescence spectra of other *cis*-1,2-diarylethenes,[8,10] and its somewhat blue-shifted origin relative to the fluorescence spectrum of *t*-APE_B is consistent with the blue-shifted origin of the absorption spectrum of the *c*-APE conformer mixture. In rigid media that preclude photoisomerization the fluorescence spectra of *c*-ATE (decalin, −150 °C)[20] and *c*-APE (MCH-3MP, −153 °C)[11] show resolved vibronic structure and are relatively red-shifted. Since for Ar-saturated solutions the major portion of the fluorescence at 20.0 °C originates from adiabatically formed ^1t-APE_B*, the fluorescence excitation spectrum of *c*-APE should track primarily the absorption spectrum of *c*-APE_B. It is not unexpected, therefore, that in toluene our fluorescence excitation spectrum in Figure 1, though similar, does not track the absorption spectrum of *c*-APE exactly. Especially large deviations, observed in the second absorption band in the 290−320-nm region, are probably not significant due to the large absorbance of the *c*-APE solution in that region ($A = 0.8$ at 296 nm). Interestingly, the reported fluorescence excitation spectrum of *c*-APE in MCH-3MP is almost identical to the *c*-APE absorption spectrum.[11] The fluorescence excitation spectra are expected to depend on the emission wavelength monitored since, based on our fluorescence spectra, the onset of *c*-APE_A absorption should be at somewhat longer wavelengths than the onset of *c*-APE_B absorption.

Fluorescence Quantum Yields. The ratio of the fluorescence quantum yields of the APE isomers, $\bar{\phi}_{f_t}/\bar{\phi}_{f_c} = 1.80$ at 366 nm, based on the static cell measurements, Figures 2 and 4, is in good agreement with the independently measured quantum yields using quinine bisulfate as fluorescence standard. Our $\bar{\phi}_{f_c}$ values, varying between 0.53 and 0.46 for λ_{exc} in the 340−390-nm range, are somewhat smaller than $\bar{\phi}_{f_c} = 0.57$ reported earlier.[2,3] This discrepancy may be due to the use of the flow cell system that eliminates the small buildup of *t*-APE that occurs in the course of spectral acquisition under static cell conditions. The substantially smaller $\bar{\phi}_{f_c} = 0.12$ obtained for $\lambda_{exc} = 410$ nm, the onset of *c*-APE absorption, is consistent with substantial *c*-APE_A absorption at that wavelength. The low $\bar{\phi}_{f_c}$ value reflects the low fluorescence quantum yield of ^1c-APE_A* (we estimate $\phi_{f_{c\text{-}A}} \simeq 0.025$, as an upper limit[23]) and the failure of this conformer to undergo adiabatic isomerization to the highly fluorescent ^1t-APE_A*.

Earlier extensive measurements of $\bar{\phi}_{f_t}$ under the same conditions (toluene, 20 °C) had yielded values in the 0.76−0.83 range for $340 \le \lambda_{exc} \le 372$ nm.[16a] As x_A, the fractional contribution of *t*-APE in the fluorescence spectrum, increases at $\lambda_{exc} \ge 400$ nm, the reported $\bar{\phi}_{f_t}$'s approach unity.[16a] The relationship of these $\bar{\phi}_{f_t}$ to $\bar{x}_A$

$$\frac{1}{\bar{\phi}_{f_t}(\lambda_{exc})} = \frac{1}{\phi_{f_{t\text{-}B}}} + \left(\frac{1}{\phi_{f_{t\text{-}A}}} - \frac{1}{\phi_{f_{t\text{-}B}}}\right) x_A(\lambda_{exc}) \qquad (5)$$

was used to estimate $\phi_{f_{t\text{-}B}} = 0.81$ and $\phi_{f_{t\text{-}A}} = 1.00$ as the conformer specific fluorescence quantum yields.[16a,18a] However, it was pointed out that a significant deviation of the $\bar{\phi}_{f_t}$'s from the plot of $\bar{\phi}_{f_t}^{-1}$ vs x_A could reflect either uncertainty in the $\bar{\phi}_{f_t}$'s or a λ_{exc} dependence of $\phi_{f_{t\text{-}B}}$ and, possibly, of $\phi_{f_{t\text{-}A}}$.[18a] Viewed in this context, our experimental $\bar{\phi}_{f_t} = 0.89$ at $\lambda_{exc} =$ 340 and 344 nm leads to a tentative preference for the former explanation. Used in eq 5 together with the earlier $\bar{\phi}_{f_t}$'s for $\lambda_{exc} \ge 400$ nm we obtain $\phi_{f_{t\text{-}A}} = 1.00$, as before,[16a,18a] and a somewhat larger $\phi_{f_{t\text{-}B}} = 0.88$, independent of λ_{exc}. Since $x_A = 0.12$ for $\lambda_{exc} = 366$ nm,[18a] eq 5 predicts $\bar{\phi}_{f_t} = 0.89_3$ which leads to $\bar{\phi}_{f_c} = 0.49_6$ based on the analysis of the spectra in Figure 2.

Conformer-Specific Photochemistry. The fluorescence spectra of *c*-APE in Ar-saturated toluene obtained for the quantum yield determinations for $\lambda_{exc} = 340$, 350, and 360 nm are nearly identical. Based on the resolved spectra in Figure 1, they correspond to 74.5 ± 0.3% ^1t-APE_B* and 25.5 ± 0.3% ^1c-APE* fluorescence contributions. It follows that the effective quantum yields of the two components are $\phi_{f_{tc}} = 0.131 \pm 0.002$ and $\phi_{f_{t\text{-}B}} = 0.383 \pm 0.013$ for these three excitation wavelengths. As pointed out above, significantly larger contributions for ^1c-APE* emission are observed as λ_{exc} approaches the onset (∼410 nm) of *c*-APE absorption indicating that excitation of *c*-APE_A, which does not undergo detectable adiabatic $^1c^* \rightarrow {}^1t^*$ isomerization, is relatively more effective at higher λ_{exc}. The inefficiency of the $^1c^* \rightarrow {}^1t^*$ isomerization process for c-APE_A can be appreciated by considering the location in Figure 6 of the combination coefficients of the fluorescence spectrum of the Ar-saturated solution excited at 410 nm. It is reflected in the deviation of points from the three-component plane defined by the triangle in Figure 6. Despite the fact that, due to larger absorptivities of the *t*-APE's,[18] fluorescence spectra obtained for this λ_{exc} are especially sensitive to the presence of *t*-APE as an impurity (see points in Figure 6 for the solution contaminated with 5% *t*-APE), the point for the pure *c*-APE solution falls very close to the ^1c-APE*/^1t-APE_B* side of the triangle. Based on 0.88 as the fluorescence quantum yield of ^1t-APE_B*, competitive absorption of incident light by *c*-APE_A ensures that at least 44% of ^1c-APE_B* undergoes adiabatic isomerization to ^1t-APE_B*.[22] Intersystem crossing from ^1t-APE_B* should, therefore, contribute significantly to the yield of triplets observed on excitation of *c*-APE.[3] Thus, substitution of the 2-anthryl group for one of the phenyl groups in stilbene markedly enhances the efficiency of adiabatic isomerization on the lowest excited singlet state surface of only one of the APE conformers in toluene, Scheme 1. Aside from the larger enhancement of the conformer specific adiabatic $^1c^* \rightarrow {}^1t^*$ pathway, *c*-APE and *c*-NPE exhibit entirely analogous behavior.[10] The analogy with *c*-APE can be extended further if we consider photocyclization to dihydrophenanthrenes. Conformer-specific photocyclization

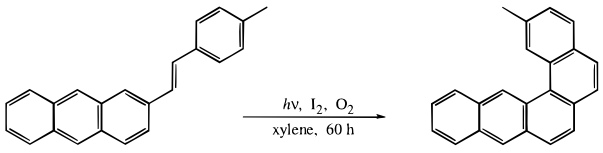

of *c*-NPE_A has been reported by several workers.[24] Conformer-specific photocyclization of *c*-APE_A can be inferred from a single report on the ATE derivative. Prolonged irradiation of

(23) It is assumed that absorption at $\lambda_{exc} = 374$ nm is primarily by *c*-APE_B. It follows that the ratio of resulting ^1c-APE_B* to ^1t-APE_B* fluorescence is at least 1:3.1. Subtraction of the ^1t-APE_B* (60%) and ^1c-APE_B*(19%) contributions from the *c*-APE spectrum for $\lambda_{exc} = 410$ nm gives 0.025 as the quantum yield of the residual ^1c-APE_A* fluorescence.

(24) See the following reviews and references cited therein: (a) Muszkat, K. A. *Top. Curr. Chem.* **1980**, *88*, 89−144. (b) Mallory, F. B.; Mallory, C. W. *Org. React.* **1984**, *30*, 1−456. (c) Laarhoven, W. H. *Photochromism, Molecules and Systems;* Dürr, H., Bouas-Laurent, H., Eds.; Elsevier: Amsterdam, 1990; pp 270−313.

t-ATE under oxidative conditions gives a 15% yield of the phenanthrene corresponding to the cyclization of ^1c-ATE$_A$*, as the only isolable product.[25] Assuming the usual mechanism for the formation of the above phenanthrene derivative reveals further that the photoisomerization of ATE cannot be exclusively one way. A minor pathway must exist in the t → c direction. Preliminary observations indicate that, under the conditions described for Figure 2, the photostationary state, though not exactly 100% *t*-APE, is >99% *t*-APE.

We recently obtained a rough estimate of the fluorescence lifetime, $\tau_{f_c} \simeq 4 \pm 1$ ps, for ^1c-NPE* based on its fluorescence quantum yield and an estimated radiative rate constant, k_{f_c}.[10] The fact that the fluorescence lifetime of ^1c-APE* is three orders of magnitude longer is, no doubt, a reflection of the greater degree of localization of the excitation in the larger aryl substituent. Such localization might diminish the ability of ^1c-APE* to undergo radiationless decay via the large-amplitude torsional motions of the olefinic portion of the molecule that are essential for cis → trans isomerization. Other radiationless decay paths, such as intersystem crossing, might be expected to compete more effectively in ^1c-APE* than in ^1c-NPE*. The much higher efficiency of the ^1c_B* → ^1t_B* adiabatic reaction in ^1c-APE* is therefore all the more noteworthy.

The fluorescence lifetime of *c*-APE is highly medium dependent. The decrease from 4.5 ns in toluene at 20 °C to 2 ns in fluid MCH-3MP is difficult to interpret because ϕ_{fc} is unknown under the latter conditions.[11] The estimated low value, ~0.025, for the effective quantum yield of ^1c-APE$_A$*, even when preferential excitation of this conformer is achieved by employing λ_{exc} at the onset of *c*-APE absorption, suggests that the bulk of *c*-APE fluorescence can be assigned to ^1c-APE$_B$*. It follows that $\phi_{f_c} \simeq 0.13 \pm 0.01$, although a lower limit, should be very close to the fluorescence quantum yield of *c*-APE$_B$. If we assign our τ_{f_c} to this conformer, we obtain $k_{f_c} = 2.9 \times 10^7$ s^{-1} for the radiative rate constant of ^1c-APE* in toluene. A dramatic increase of τ_{f_c} to 90 ns in MCH-3MP at 77 K can probably be attributed in part to the suppression of torsional motion in the glassy medium.[11] It is surprising, however, that the estimated $k_{f_c} = 5 \times 10^6$ s^{-1} under these conditions[11] is nearly six times smaller than our value for toluene at 20 °C. The usual dependence of k_f on the refractive index cannot account for such a large change.[26] It appears that either most of ^1c-APE* fluorescence originates from a different conformer in fluid solution than in the glassy medium or, if the same conformer persists as the major source of the fluorescence, its emission reflects the coupling of more than one excited state. Diminished coupling with a state with a more allowed radiative transition could account for the decrease in the effective radiative rate constant at low temperature. Strong evidence demonstrating coupled decay of the two lowest excited singlet states of *t*-APE$_B$ has been presented.[16]

The effective radiationless decay rate constant of ^1c-APE* in toluene at 20 °C is $k_{nr_c} = 2 \times 10^8$ s^{-1}. Since this rate constant can be assigned mainly to torsional motion along the ^1c_B* → ^1t_B* adiabatic reaction coordinate, the activation energy barrier along this coordinate may be as high as 7 kcal/mol.[27] Whether this barrier is on the way to a shallow minimum at the perpendicular geometry, ^1p_B*, or whether ^1p_B* corresponds to the geometry of the transition state for the ^1c_B* → ^1t_B* process, as appears to be the case on the lowest triplet state energy surface,[1−3] remains to be established. Transient absorption measurements and medium and temperature effects on the fluorescence and photochemistry of *c*-APE are in progress.

Acknowledgment. This research was supported by NSF Grant No. CHE 93-12918.

JA951630H

(25) Laarhoven, W. H.; Cuppen, Th. J. H. M.; Nivard, R. J. F. *Tetrahedron* **1970**, 4865−4881.

(26) Saltiel, J.; Waller, A. S.; Sears, D. F., Jr.; Garrett, C. Z. *J. Phys. Chem.* **1993**, *97*, 2516−2522 and references cited therein.

(27) The Arrhenius *A* factor of ^1c-NPE* [10] was employed in this estimation.